Intermetallics 17 (2009) 945–950

Contents lists available at ScienceDirect

Intermetallics

journal homepage: www.elsevier.com/locate/intermet

Microstructure and electrochemical behavior of Ti-coated $Zr_{55}Al_{10}Ni_5Cu_{30}$ bulk metallic glass

F.X. Qin [a,*], X.M. Wang [a], G.Q. Xie [a], K. Wada [a], M. Song [b], K. Furuya [b], K. Asami [a], A. Inoue [a]

[a] Institute for Materials Research, Tohoku University, Sendai 980-8577, Japan
[b] National Institute for Materials Science, Tsukuba 305-0003, Japan

ARTICLE INFO

Article history:
Received 11 September 2008
Received in revised form
19 November 2008
Accepted 22 April 2009
Available online 24 May 2009

Keywords:
B. Glasses, metallic
C. Coatings, intermetallics and otherwise
C. Nanocrystals
F. Electrochemical characterization
G. Biomedical applications

ABSTRACT

In this study, pure Ti was coated on $Zr_{55}Al_{10}Ni_5Cu_{30}$ bulk metallic glass (BMG) using a physical vapour deposition (PVD) technique with magnetron sputtering. Microstructures of Ti coating, BMG substrate and interface were investigated by conventional and high-resolution transmission electron microscopy (TEM and HREM). The electrochemical behavior of Ti-coated $Zr_{55}Al_{10}Ni_5Cu_{30}$ BMG was studied by potentiodynamic polarization curves and electrochemical impedance spectroscopy (EIS) in Hanks' solution. Scanning electron microscopy (SEM) was used to characterize the surface morphology of the coating after electrochemical testing. HRTEM observation reveals that the sputtering Ti coating consists of α-Ti nano-scale particles with the size about 10 nm. The polarization curves revealed that the open-circuit potential shifted to a more positive potential and the passive current density was lower after Ti coating was applied in comparison with that of the monolithic $Zr_{55}Al_{10}Ni_5Cu_{30}$ BMG. Electrochemical impedance spectroscopy (EIS) measurements showed that the Bode plots of Ti-coated $Zr_{55}Al_{10}Ni_5Cu_{30}$ BMG presented one time constant for 1 h and 12 h immersion and two time constants after 24 h immersion. The good bonding condition between Ti coating and $Zr_{55}Al_{10}Ni_5Cu_{30}$ BMG substrate may be responsible for the high corrosion resistance of Ti-coated $Zr_{55}Al_{10}Ni_5Cu_{30}$ BMG.

1. Introduction

Bulk metallic glasses (BMGs) have attracted much attention as a new material due to their unique characteristics (high mechanical strength, low Young's modulus, large elastic elongation, high fracture toughness, good corrosion resistance etc.), which cannot be obtained for conventional crystalline materials [1–4]. The BMGs exhibit high corrosion resistance owing to their structural disorder and chemical homogeneity. They do not contain crystalline defects, such as grain boundaries or dislocations acting as preferential sites for corrosion. Thus, the glassy state provides the formation of a uniform passive film without weak points with respect to corrosion and presents better corrosion properties than the crystalline counterparts with the same component in many alloy systems [5]. Zr–Al–Ni–Cu alloy system is known as the best glass-forming system as is evident from the large critical diameter of 30 mm [6,7]. Zr–Al–Ni–Cu and Zr–Ti–Al–Ni–Cu bulk glassy alloys exhibit high glass-forming ability and good mechanical properties. High bending fracture strength of 3000–3900 MPa, which is 2–2.5 times higher than those of crystalline Zr-based and Ti-based alloys, was reported [8]. Moreover, applications of Zr–Al–Ni–Cu BMG require high chemical stability in various environments in order to ensure an acceptable lifetime. Zr–Al–Ni–Cu BMGs have been proposed to be applied in orthopaedics and dental surgery, because of excellent mechanical properties and high polarization resistance in an artificial body fluid [9]. However, recently the authors [10] found that Zr-based BMGs had almost no apatite-forming ability after alkali-treatment, although Zr metal was reported to have apatite-forming ability after certain treatments [11]. Moreover, the toxicity of alloy elements (Ni, Cu or Al) in the glass also restricts the biomedical applications due to the possibility of causing an allergy reaction, cancer or other diseases in human body.

On the other hand, surface coating produced by PVD method is a useful technique to improve the surface properties of metallic materials such as wear resistance, anti-corrosion properties and oxidation resistance [12–15]. It has been widely applied in steels [12] and magnesium alloys [13]. Additionally, PVD method has already been used in investigating medical materials. Liu et al. [15] reported that PVD TiN coating on Ti–6Al–4V alloy as artificial hip joints is effective to enhance wear resistance and corrosion performance. So far rare data on PVD-coated BMGs were published. To utilize both the advantages of BMGs in mechanical properties

* Corresponding author. Tel.: +81 22 215 2592; fax: +81 22 215 2381.
E-mail address: fxqin@imr.tohoku.ac.jp (F.X. Qin).

0966-9795/$ – see front matter © 2009 Elsevier Ltd. All rights reserved.
doi:10.1016/j.intermet.2009.04.009

(high strength, low Young's modulus and high elasticity) and the advantages of PVD coatings (wear resistance, chemical inertness and high thermal stability), the PVD coating technique is employed in this study. Ti was chosen because Ti has very good corrosion resistance in Cl^--containing solution. Ti is also a good biocompatible material and its surface osteo-conductivity can be improved through hydroxyapatite coating by alkaline treatments. Furthermore, Ti coating is expected to prohibit the dissolution of Ni, Al and Cu ions and improve the corrosion resistance and bioactivity of the Zr-based BMGs.

Combining superior electrochemical properties of PVD coating with excellent mechanical properties of BMGs, the BMGs could be qualified candidates for medical applications. In this study, Ti coating on $Zr_{55}Al_{10}Ni_5Cu_{30}$ BMG was prepared by means of magnetic sputtering. The microstructure and electrochemical properties in Hanks' solution of Ti-coated $Zr_{55}Al_{10}Ni_5Cu_{30}$ BMG were investigated.

2. Experimental procedure

Master ingots of $Zr_{55}Al_{10}Ni_5Cu_{30}$ alloy (composition is given in nominal at.%) were prepared by arc melting the mixture of pure metals (>99.9 mass%) in an argon atmosphere. The substrate BMG samples in a plate form with dimension of 1 mm × 15 mm × 50 mm were prepared by injection casting into copper mold. Before the deposition process, the $Zr_{55}Al_{10}Ni_5Cu_{30}$ BMG substrates were finely polished with SiC paper and Al_2O_3 paste, ultrasonically washed in distilled water and acetone, then dried in air. After the chamber was evacuated to a pressure of 6×10^{-3} Pa, argon was introduced. Afterwards, Ti was deposited on the $Zr_{55}Al_{10}Ni_5Cu_{30}$ BMG substrates by evaporation of pure Ti cathode with the substrate temperature of about 200 °C using a direct current magnetron sputtering system. The deposition parameters were as follows: Voltage of 350 V, beam current of 6.0–10.0 A and deposition time of 5 min. The structure of Ti-coated $Zr_{55}Al_{10}Ni_5Cu_{30}$ BMG was examined by micro-area X-ray diffraction with Co Kα radiation (XRD, Bruker, D 8 Discover GADDS). The microstructures of Ti sputter coating, substrate and interface were investigated by conventional and high-resolution transmission electron microscopy (TEM and HRTEM). The TEM samples were prepared by using a JEOL JEM-9310 focused ion beam (FIB) system.

The electrochemical behavior of the samples was evaluated by potentiodynamic polarization and electrochemical impedance spectroscopy (EIS) in Hanks' solution at 37 °C. The composition of Hanks' solution (g/l) is 8.00 NaCl, 0.40 KCl, 0.35 $NaHCO_3$, 0.19 $CaCl_2 \cdot 2H_2O$, 0.09 $Na_2HPO_4 \cdot 7H_2O$, 0.2 $MgSO_4 \cdot 7H_2O$, 0.06 KH_2PO_4 and 1.00 glucose. Electrochemical measurements were conducted in a three-electrode cell using a platinum plate as counter electrode and a saturated calomel reference electrode (SCE) as reference electrode. Potentiodynamic polarization curves were measured with a potential sweep rate of 0.83×10^{-3} V/s after immersing the specimens for 600 s. EIS was also measured at open-circuit potential, with a frequency range from 10^5 to 10^{-2} Hz, and an amplitude perturbation of 10 mV.

3. Results

3.1. Structure of Ti coating and interface

Fig. 1 shows the XRD pattern of Ti coating on $Zr_{55}Al_{10}Ni_5Cu_{30}$ BMG substrate. Ti coating on $Zr_{55}Al_{10}Ni_5Cu_{30}$ BMG exhibits a single nano-phase of α-Ti. In order to confirm the detailed microstructure of Ti coating, TEM and HRTEM were carried out. Fig. 2 shows the bright-field TEM image taken from the interfacial region between Ti coating and BMG substrate. Ti coating exhibits grey contrast with

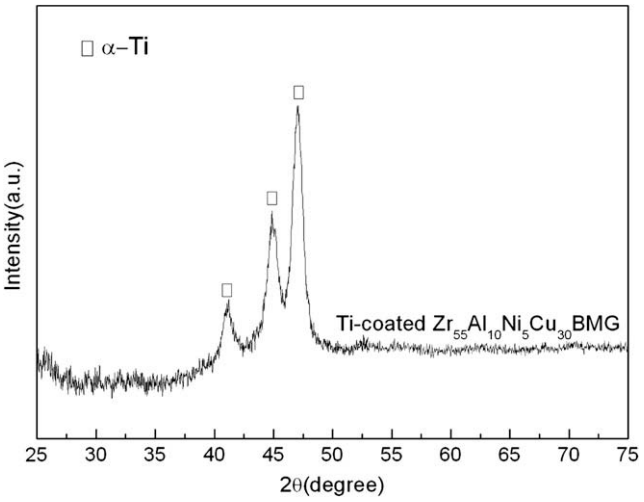

Fig. 1. XRD patterns of Ti coatings on $Zr_{55}Al_{10}Ni_5Cu_{30}$ BMG substrate.

a thickness of about 500 nm, while the BMG substrate shows a dark contrast. No defects such as separation are observed at the interface between Ti coating and BMG substrate, indicating that there is a highly dense coating and good interface bonding state. Fig. 3(a)–(c) shows HRTEM micrographs and the corresponding selected-area diffraction (SAD) patterns taken from coating, interface and substrate, respectively. HRTEM observation reveals that Ti coating consists of nano-scale particles with the size about 10 nm, as shown in Fig. 3(a). The nano-particles are identified as a hexagonal α-Ti structure from the SAD patterns, the fringe spacing and the geometry of crossed-fringe image. Good bonding between Ti coating and BMG substrate is confirmed in Fig. 3(b). In addition, a halo electron diffraction pattern was taken from BMG substrate shown in Fig. 3(c), suggesting that $Zr_{55}Al_{10}Ni_5Cu_{30}$ substrate retains a full glassy state. No change is found after Ti sputtering on the BMG substrate, i.e. the sputtering process at 200 °C has no influence on the microstructure of BMG substrate.

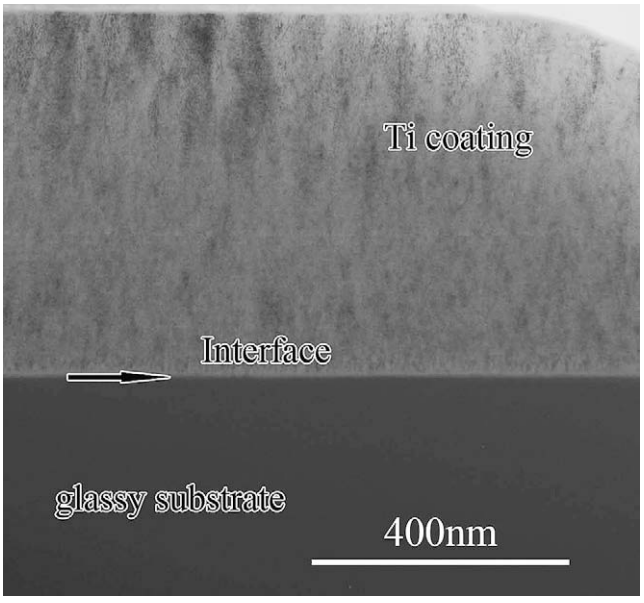

Fig. 2. Bright-field TEM image of Ti coating on $Zr_{55}Al_{10}Ni_5Cu_{30}$ BMG substrate.

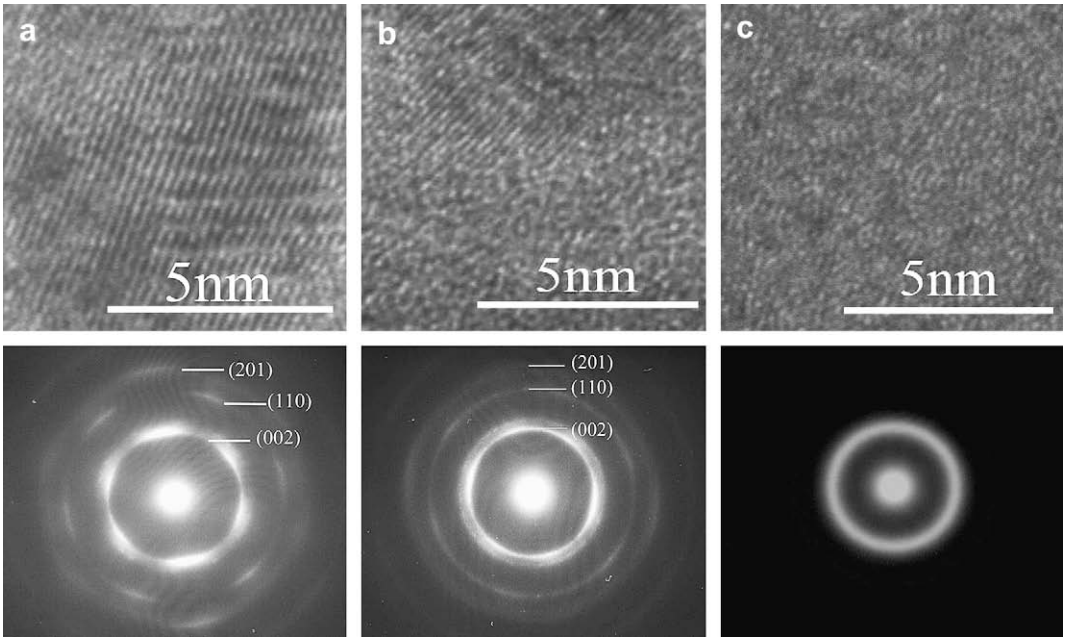

Fig. 3. HRTEM images and the corresponding SAD patterns of Ti coating (a), interface (b) and $Zr_{55}Al_{10}Ni_5Cu_{30}$ BMG substrate (c).

3.2. Potentiodynamic polarization curves

Fig. 4 shows polarization curves of Ti-coated $Zr_{55}Al_{10}Ni_5Cu_{30}$ BMG and the monolithic $Zr_{55}Al_{10}Ni_5Cu_{30}$ BMG in Hanks' solution. Within the anodic polarization region, the passive current density of the monolithic $Zr_{55}Al_{10}Ni_5Cu_{30}$ BMG is higher than that of Ti-coated $Zr_{55}Al_{10}Ni_5Cu_{30}$ BMG sample. Ti-coated $Zr_{55}Al_{10}Ni_5Cu_{30}$ BMG shows a more noble open-circuit potential of about −200 mV in comparison to that of the monolithic $Zr_{55}Al_{10}Ni_5Cu_{30}$ BMG, −320 mV. The passive current density of Ti-coated $Zr_{55}Al_{10}Ni_5Cu_{30}$ BMG is located at between 10^{-3} and 10^{-4} A/m^2, which is one or one and a half order of magnitudes lower than that of the monolithic $Zr_{55}Al_{10}Ni_5Cu_{30}$ BMG. The passive current density of $Zr_{55}Al_{10}Ni_5Cu_{30}$ BMG coated by titanium dramatically decreases due to the passivation of Ti coating [13]. Ti coating can separate the $Zr_{55}Al_{10}Ni_5Cu_{30}$ BMG from the solution protecting the BMG substrate from corrosion. Consequently, Ti-coated $Zr_{55}Al_{10}Ni_5Cu_{30}$ BMG exhibited lower passive current density than the monolithic $Zr_{55}Al_{10}Ni_5Cu_{30}$ BMG.

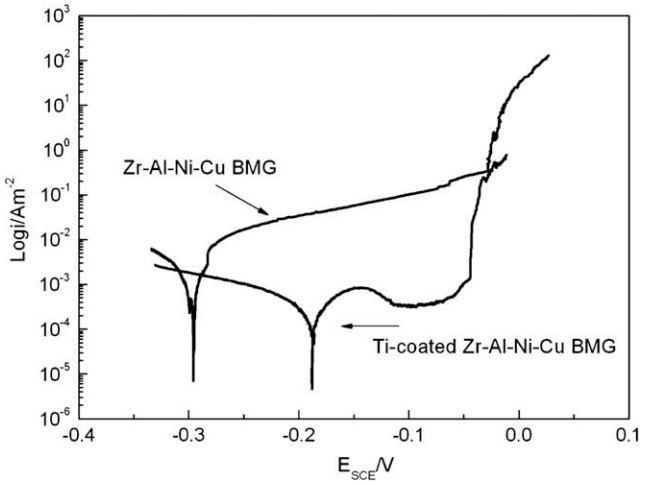

Fig. 4. Polarization curves of Ti-coated $Zr_{55}Al_{10}Ni_5Cu_{30}$ BMG and the monolithic $Zr_{55}Al_{10}Ni_5Cu_{30}$ BMG in Hanks' solution.

3.3. Electrochemical impedance spectroscopy

Potentiodynamic polarization studies are fast and destructive and not sufficient to explain the corrosion mechanism that takes place at the electrolyte/coating/metal interface [16]. In addition, the EIS technique does not significantly accelerate the corrosion reactions due to only a small amplitude sinusoidal signal throughout the electrode system. Thereby the coating surface is not affected seriously and EIS is considered to be a useful and non-destructive method for coating materials.

Fig. 5 shows Bode plots of Ti-coated $Zr_{55}Al_{10}Ni_5Cu_{30}$ BMG at open-circuit potential for different immersion times. Impedance data at high frequencies usually represent the responses of coating, exhibiting the coating characteristics. Bode plot (phase angle, φ vs. log f) in Fig. 5 for Ti-coated $Zr_{55}Al_{10}Ni_5Cu_{30}$ BMG shows one single and broad peak after 12 h immersion, indicating one time constant for the corrosion process at the solution/coating interface [17]. Ti coating prevents pitting corrosion to $Zr_{55}Al_{10}Ni_5Cu_{30}$ BMG substrate by forming a protective titanium oxide. On increasing the immersion time to 24 h, phase angle vs. log f plot shows two peaks for Ti-coated $Zr_{55}Al_{10}Ni_5Cu_{30}$ BMG, hinting that two interfaces are present due to the pitting corrosion. The electrochemical interface can be subdivided into two sub-interfaces, i.e., solution/coating interface and solution/substrate interface at pinholes. With further immersion up to 48 h, impedance absolute values, $|Z|$, slightly increased due to the blocking of corrosion products in pinholes.

3.4. Surface morphologies

After the completion of potentiodynamic polarization testing, the surface morphologies of Ti-coated $Zr_{55}Al_{10}Ni_5Cu_{30}$ BMG sample were observed by scanning electron microscopy (SEM) equipped with X-ray energy dispersive spectroscopy (EDS), and the corresponding results are shown in Fig. 6. One deep pit on the surface of Ti-coated $Zr_{55}Al_{10}Ni_5Cu_{30}$ BMG was observed (Fig. 6(a)).

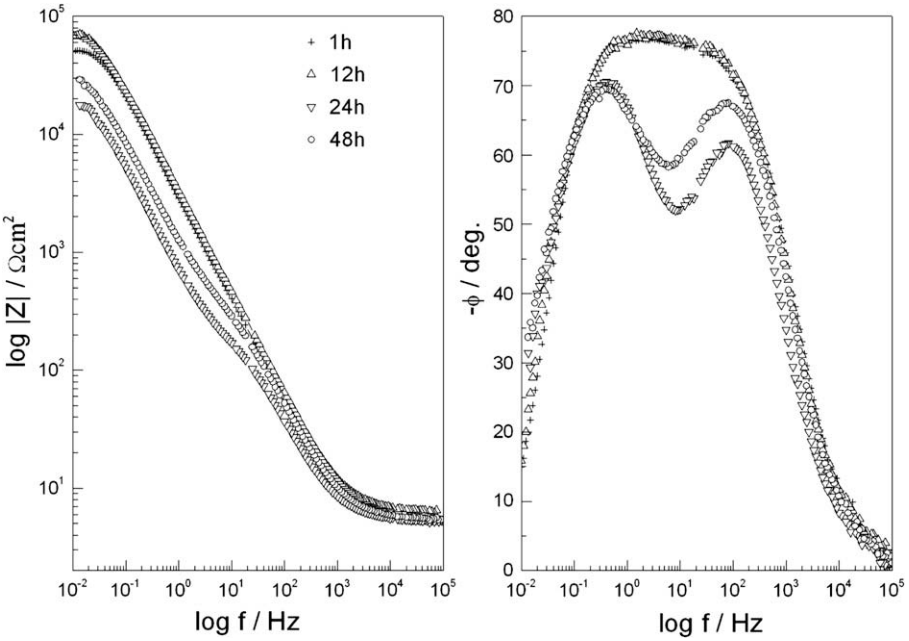

Fig. 5. Bode plots of EIS data for Ti-coated $Zr_{55}Al_{10}Ni_5Cu_{30}$ BMG in Hanks' solution at different immersion times.

Ti originated from sputtering is obviously detected on the surface around the outer part of pit in Fig. 6(b). The pit region was rich in Cu and Zr, indicating the formation of oxides of Cu, Zr and O as mainly corrosion products over the pit, as presented in Fig. 6(c)–(e).

4. Discussion

Interpretation of the EIS data with an appropriate equivalent circuit can provide detailed information on the electrochemical reaction that takes place on the electrode. From the EIS data, the resistance of pores in the coating (R_{pore}) and the charge transfer resistance (R_{ct}), the electrical double-layer capacitance at the solution/coating interface (C_{coat}) as well as the electrical double-layer capacitance at the solution/substrate interface (C_{dl}) can be obtained. The equivalent circuit shown in Fig. 7(a) is used to model the EIS data with one time constant, and Fig. 7(b) is usually used for EIS modeling with two time constants. Here, R_e is electrolyte resistance, which depends on the distance between working electrode (WE) and the tip of reference electrode (RE). A constant phase angel element (CPE) is used to replace a capacitance because it hardly has pure capacitance in real electrochemical process. It is defined as $Q = 1/Y_o\,(j\omega)^n$. Here, n is dimensionless number, which has a value $0 \le n \le 1$, which can be obtained from the slope of $|Z|$ on the Bode plot. Y_o is associated with the roughness of the electrode surface. The corresponding simulated data are listed in Table 1. It is known [16–19] that the parallel RC circuit represents a time constant (τ), corresponding to a characteristic frequency ω_c which is defined by $\tau = 1/\omega_c = 1/RC$. The parameters of R_{pore} and Q_{coat} are related to the properties of the coating/solution interface reactions. R_{ct} and Q_{dl} are associated with the charge transfer

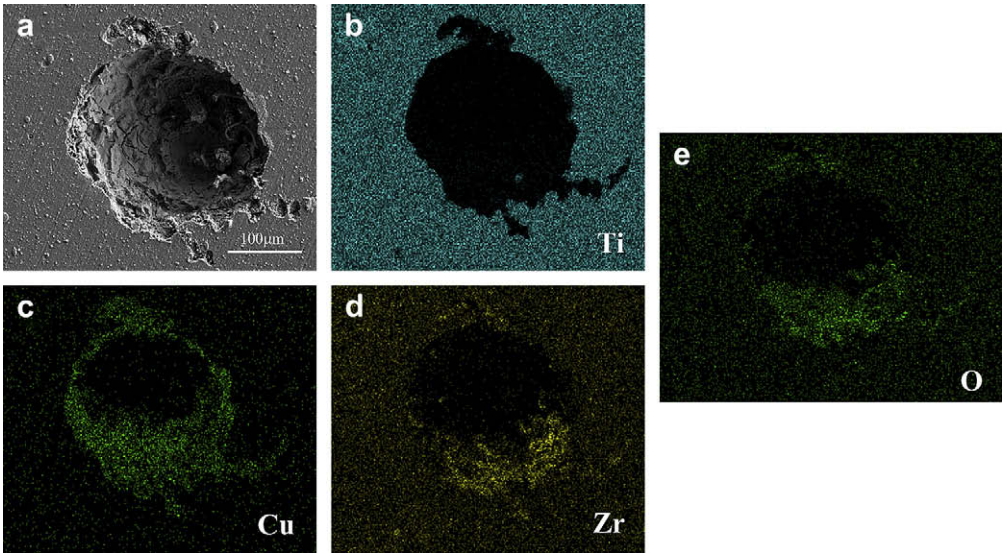

Fig. 6. SEM image (a) and X-ray mappings (b–e) of Ti-coated $Zr_{55}Al_{10}Ni_5Cu_{30}$ BMG polarization test.

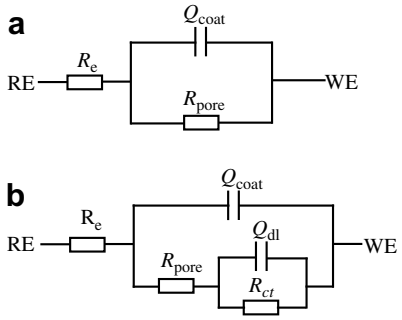

Fig. 7. Equivalent circuits for Ti-coated $Zr_{55}Al_{10}Ni_5Cu_{30}$ BMGs in Hanks' solution, (a) one time constant (b) two time constants.

reactions at the solution/substrate interface. For Ti-coated $Zr_{55}Al_{10}Ni_5Cu_{30}$ BMG, the impedance value increased slightly due to the passivity of Ti coating after 12 h immersion as shown in Fig. 5(a) and Table 1, with the R_{ct} value of the order of $10^5\ \Omega\ cm^2$ and $Q_c - Y_0$ of the order of 10^{-6} F/cm^2. The BMG substrate is a relatively passive substrate. The electrochemical response of BMG is hardly distinguishable from that of Ti coating [18]. Hence, at initial period of immersion and short time immersion (1 h and 12 h), only one time constant exists, which represents the overall surface, Ti coating and the passive films on the BMG at pores. The second time constant related to the solution/substrate interface via pinholes was observed after 24 h immersion as shown in Fig. 5(b), suggesting that the solution had penetrated the coating through pinholes and the galvanic corrosion cells had established [19]. Corrosion of coating materials is usually localized at the pores, pinhole or void, where the corrosive solution is able to penetrate into the substrate [18]. The coating behavior is as a leaky capacitor. The case is even more severe if the coating systems are exposed to an aggressive environment, for example, a Cl^--containing solution due to the aggressive effects of chloride ion in promoting pitting corrosion. On further increasing the immersion time, the impedance enhanced slightly after 48 h immersion as compared to 24 h immersion induced by the blocking of pinholes by corrosion products [20] from the solution/substrate interface. That is, after 48 h immersion, the corrosion products plugged in the pinholes and the electric resistances of corrosion products were higher than that of solution. Thus, a little higher impedance was induced compared with early pitting period of 24 h immersion.

It is well known that PVD coatings exhibit good wear resistance, chemical inertness and high thermal stability [14]. But, the coatings produced by the PVD method often exhibit porosity, which can't be absolutely avoided. The corrosion in PVD coatings takes place preferentially through pinholes, voids or other defects, which provide an easy fracture path for adhesion failure, allowing contact of the substrate with electrolyte [21,22]. In order to lessen the coating defects and enhance the corrosion resistance, many researchers have devoted themselves to adjusting deposition parameters [23] or preparing multilayer coatings [24–30]. Interfacial integrity and adhesion of the PVD coatings are considered to be important properties and can be enhanced by the presence of an appropriate interlayer. Among them, a Ni–P amorphous interlayer appeared to be more effective [31–33]. In this research, it is proposed that the $Zr_{55}Al_{10}Ni_5Cu_{30}$ substrate in a glassy state also offer positive effect to the corrosion resistance. A general feature of sputtering coating is that, after the original nucleation stage, the growth takes place in isolated islands which then grow together leaving voids between them [13]. It can be proposed that less defect coating is expected on a uniform substrate. The metallic glasses are uniform in chemical composition and structure, providing more homogeneous, uniform and dense microstructure of the coating. Therefore, the Ti coating on the $Zr_{55}Al_{10}Ni_5Cu_{30}$ glassy substrate is expected to have a good corrosion resistance. However, it still shows pitting because of some defect in the sputtering Ti layer. The defects may come from incomplete cleaning of the surface and be related to a vacuum coating process. The surface cleanliness of the BMG substrate should be improved to further inhibit pitting corrosion. Furthermore, it is worthy to notice that good bioactivity of Ti coating $Zr_{55}Al_{10}Ni_5Cu_{30}$ BMG was also obtained by two-step chemical treatment method [10]. In a sense, Ti-coated $Zr_{55}Al_{10}Ni_5Cu_{30}$ BMG has an attractive potential application as biomaterials in various medical fields.

Table 1
EIS data obtained by equivalent simulation of Ti-coated $Zr_{55}Al_{10}Ni_5Cu_{30}$ BMG.

Exposed time	R_s (Ω cm^2)	$Q_{coat} - Y_0$ (μF/cm^2)	n_c	R_{pore} (Ω cm^2)	$Q_{dl} - Y_0$ (μF/cm^2)	n_{dl}	R_{ct} (Ω cm^2)
1 h	8.5	3.54	0.94	4.74×10^5	–	–	–
12 h	9.2	2.74	0.92	6.75×10^5	–	–	–
24 d	5.5	0.42	0.74	7.09×10^3	6.79	0.97	2.50×10^5
48 d	5.1	0.68	0.83	1.10×10^4	6.12	0.96	2.76×10^5

5. Conclusions

Ti coating consisting of α-Ti nano-phase was deposited on $Zr_{55}Al_{10}Ni_5Cu_{30}$ BMG by magnetic sputtering. The polarization curves and EIS revealed that higher corrosion resistance has been obtained for the Ti-coated $Zr_{55}Al_{10}Ni_5Cu_{30}$ BMGs compared with the monolithic $Zr_{55}Al_{10}Ni_5Cu_{30}$ BMG in Hanks' solution. Open-circuit potentials shifted to a more positive potential and the passive current densities were lower after the Ti coating was applied comparing with that of the monolithic $Zr_{55}Al_{10}Ni_5Cu_{30}$ BMG substrate. Passive current densities were about one or one and a half order of magnitude lower than that of the uncoated $Zr_{55}Al_{10}Ni_5Cu_{30}$BMG. The Bode plots present one time constant for Ti-coated $Zr_{55}Al_{10}Ni_5Cu_{30}$ BMG immersion for 12 h, while two time constants for Ti-coated $Zr_{55}Al_{10}Ni_5Cu_{30}$ BMG after a long-time immersion. No crystallization of the BMG substrate and the good bonding state between the coating and substrate should be responsible for good corrosion resistance and high impedance value of Ti-coated $Zr_{55}Al_{10}Ni_5Cu_{30}$ BMG. To further prevent local corrosion, the surface cleanliness of the BMG substrate should be improved.

Acknowledgments

This work is financially supported by Research and Development Project on Advanced Metallic Glasses Inorganic Materials and Joining Technology, Institute for Materials Research, Tohoku University. Partial work was supported by "Nanotechnology Support Project" of the Ministry of Education, Culture, Sports, Science and Technology (MEXT), Japan.

References

[1] Inoue A, Ohtea K, Masumoto T. Jpn J Appl Phys 1988;27:L2248.
[2] Inoue A, Zhang T, Masumoto T. Mater Trans JIM 1989;30:965.
[3] Perker A, Johnson WL. Appl Phys Lett 1993;63:2342.
[4] Inoue A. Bulk amorphous alloys. Zurich: Trans. Tech. Publications; 1998.
[5] Gebert A, Buchholz K, Leonhard A, Mummert K, Eckert J, Schultz L. Mater Sci Eng A 1999;267:294.
[6] Inoue A, Nakamura T, Sugita T, Zhang T, Masumoto T. Mater Trans JIM 1993;34:351.
[7] Inoue A. Mater Trans JIM 1995;36:866.
[8] Inoue A. Acta Mater 2000;48:279.
[9] Hiromoto S, Tsai AP, Sumita M, Hanawa T. Corros Sci 2000;42:1651.
[10] Qin FX, Wang XM, Inoue A. Intermetallics 2008;16:917.
[11] Uchida M, Kim HM, Miyaji F, Kokubo T, Nakamura T. Biomaterials 2002;23:313.

[12] Yashar PC, Sproul WD. Vacuum 1999;55:179.
[13] Altun H, Sen S. Mater Des 2006;27:1174.
[14] Sproul WD, Graham ME, Wong MS, Rudnik PJ. Surf Coat Technol 1993;61:139.
[15] Liu C, Bi Q, Matthews A. Surf Coat Technol 2003;163–164:597.
[16] William Grips VK, Ezhil Selvi V, Barshilia HC, Rajam KS. Electrochim Acta 2006;51:3461.
[17] Liu C, Bi Q, Leyland A, Matthews A. Corros Sci 2003;45:1257.
[18] Liu C, Bi Q, Leyland A, Mathews A. Corros Sci 2003;45:1243.
[19] Liu C, Bi Q, Mathews A. Corros Sci 2001;43:1953.
[20] Liu C, Leyland A, Lyon S, Mattews A. Surf Coat Technol 1995;76–77:615.
[21] Park MJ, Leyland A, Mathews A. Surf Coat Technol 1990;43–44:481.
[22] Mantyla TA, Helevirta PJ, Lepisto TT, Siitonen PT. Thin Solid Films 1985;126:275.
[23] Korhonen AS. Vacuum 1994;45:1031.
[24] Dűck A, Gamer N, Gesatzke W, Griepentrog M, Ősterle W, Sahre M, et al. Surf Coat Technol 2001;142–144:579.
[25] Barshilia HC, Prakash MS, Jain A, Rajam KS. Vacuum 2005;77:169.
[26] Yashar P, Barnett SA, Rechner J, Sproul WD. J Vac Technol A 1998;16:2913.
[27] Nordin M, Larsson M, Hogmark S. Surf Coat Technol 1998;106:234.
[28] Zhou Y, Asaki R, Soe WH, Yamamoto R, Chen R, Iwabuchi A. Wear 1999;236:159.
[29] Panjan P, Navinsek B, Cvelbar A, Zalar A, Vlcek J. Surf Coat Technol 1998;98:1497.
[30] Panjan P, Navinsek B, Cvelbar A, Zalar A, Milosev I. Thin Solid Films 1996;281–282:298.
[31] Doong JC, Duh JG, Tsai SY. Surf Coat Technol 1993;58:157.
[32] Vencovsky PK, Sanchez R, Branco JRT, Galvano M. Surf Coat Technol 1998;108–109:599.
[33] Chen JS, Duh JG, Wu FB. Surf Coat Technol 2002;150:239.